

Deep-Dup: An Adversarial Weight Duplication Attack Framework to Crush Deep Neural Network in Multi-Tenant FPGA

Adnan Siraj Rakin ^{*1}, Yukui Luo ^{*2}, Xiaolin Xu² and Deliang Fan¹

^{*} Both Authors Contributed Equally

¹Department of Electrical, Computer and Energy Engineering, Arizona State University

²Department of Electrical and Computer Engineering, Northeastern University

Abstract

The wide deployment of Deep Neural Networks (DNN) in high-performance cloud computing platforms has emerged field-programmable gate arrays (FPGA) as a popular choice of accelerator to boost performance due to its hardware reprogramming flexibility. To improve the efficiency of hardware resource utilization, growing efforts have been invested in FPGA virtualization, enabling the co-existence of multiple independent tenants in a shared FPGA chip. Such multi-tenant FPGA setup for DNN acceleration potentially exposes DNN interference task under severe threat from malicious users. This work, to the best of our knowledge, is the first to explore DNN model vulnerabilities in multi-tenant FPGAs. We propose a novel adversarial attack framework: *Deep-Dup*, in which the adversarial tenant can inject faults to the DNN model of victim tenant in FPGA. Specifically, she can aggressively overload the shared power distribution system of FPGA with malicious power-plundering circuits, achieving *adversarial weight duplication (AWD) hardware attack* that duplicates certain DNN weight packages during data transmission between off-chip memory and on-chip buffer, with the objective to hijack DNN function of the victim tenant. Further, to identify the most vulnerable DNN weight packages for a given malicious objective, we propose a generic vulnerable weight package searching algorithm, called *Progressive Differential Evolution Search (P-DES)*, which is, for the first time, adaptive to both deep learning white-box and black-box attack models. Unlike prior works only working in a deep learning white-box setup, our adaptiveness mainly comes from the fact that the proposed P-DES does not require any gradient information of DNN model. The proposed Deep-Dup is validated in a developed multi-tenant FPGA prototype, for two popular deep learning applications, i.e., Object Detection and Image Classification. Successful attacks are demonstrated in six popular DNN architectures (e.g., YOLOv2, ResNet-50, MobileNet, etc.) on three datasets (COCO, CIFAR-10, and ImageNet). The experimental results demonstrate the effectiveness of the proposed Deep-Dup attack framework. For example, Deep-Dup can successfully attack MobileNetV2

(i.e., degrade test accuracy from 70 % to lower than 0.2 %), with only ~ 2 weight package duplication out of **2.1 Million** on ImageNet dataset. ¹

1 Introduction

Machine Learning (ML), especially deep neural networks (DNN), services in high-performance cloud computing are gaining extreme popularity due to their remarkable performance in intelligent image/video recognition [1–4], natural language processing [5–7], medical diagnostics [8], malware detection [9], and autonomous driving [10, 11]. Similar to many other high-performance computing (HPC) platforms (e.g., CPU, GPU, ASIC), reconfigurable computing devices like field-programmable gate arrays (FPGA) have been widely deployed in HPC system for DNN acceleration due to their low-effort hardware-level re-programmability to adapt various DNN structures, as well as fast algorithm evolution. For example, IBM and Intel integrated FPGAs in their CPU products for acceleration purposes [12, 13]. Alongside the rapid growth of the cloud computing market and critical developments in DNN hardware acceleration, FPGA has become a significant hardware resource for public lease. Recently, the leading cloud service providers have also started integrating FPGAs into their cloud servers. For example, the Stratix-V FPGA from Intel/Altera has been deployed by the Microsoft Project Catapult for DNN acceleration [14]. Amazon also released its EC2 F1 instances equipped with programmable hardware (UltraScale+VU9P FPGAs) from Xilinx [15].

For high efficiency and performance, there have been growing efforts to support multiple independent tenants co-residing/sharing an FPGA chip over time or simultaneously [16, 17]. The *co-tenancy* of multiple users on the same FPGA chip has created a unique attack surface, where many new vulnerabilities will appear and cause dangerous results. With many hardware resources being jointly used in the multi-tenant FPGA environment, a malicious tenant can leverage

¹Corresponding Author: dfan@asu.edu

such *indirect* interaction with other tenants to implement various new attacks. However, as a relatively new computing infrastructure, as well as one of the main hardware accelerator platforms, the *security of multi-tenant FPGAs for DNN acceleration* has not been investigated in-depth.

From DNN algorithm point of view, its security has been under severe scrutiny through generating malicious input noise popularly known as *Adversarial Examples* [18–20]. Even though tremendous progress has been made in protecting DNN against adversarial examples [21–23], *neglecting fault injection-based model parameter perturbation does not guarantee the overall security of DNN acceleration in FPGA (DNN-FPGA) system*. Several prior works have effectively demonstrated depletion of DNN intelligence by tempering model parameters (i.e., weights, biases) using supply chain access [24, 25] or through popular memory fault injection techniques [26–29], which could be in general classified as *adversarial weight attack*. Adversarial weight attack can drastically disrupt the inference behavior towards the intent of a malicious party [26–30]. The large DNN model’s parameters (e.g., weights) are extensively tuned in the training process to play a key role in inference accuracy. However, almost all the existing adversarial weight attacks assume an extremely relaxed threat model (i.e., white-box), where adversary can access all DNN model parameters, like architecture and gradients. Even though it is pivotal to study white-box attacks to understand the behavior of DNN models in the presence of input or weight noise, it is also important to explore how to conduct adversarial weight attacks in a much more strict black-box setup, where attacker has no knowledge of DNN model information.

In summary, three primary challenges that we intend to solve through our proposed attack framework are i) Considering multiple tenants *co-reside* on an FPGA, can a malicious user leverage a novel attack surface to provide the luxury of perturbing DNN model parameters of victim tenant? ii) Can the adversary conduct a black-box adversarial weight attack with no knowledge of DNN model parameters, gradient, etc., instead of white-box attack used in all prior works [26, 28]? iii) Given an FPGA hardware fault injection attack scheme and a strict black-box threat model, can adversary design an efficient searching algorithm to identify critical parameters for achieving a specific malicious objective? Inspired by those challenges, we propose *Deep-Dup* attack framework in multi-tenant DNN-FPGA, which consists of two main modules: 1) a novel FPGA hardware fault injection scheme, called *adversarial weight duplication (AWD)*, leveraging power-plundering circuit to intentionally duplicate certain DNN weight packages during data transmission between off-chip memory and on-chip buffer; 2) a generic searching algorithm, called *Progressive Differential Evolution Search (P-DES)*, to identify the most vulnerable DNN weight package index and guide AWD to attack for given malicious objective. As far as we know, Deep-Dup is the first work demonstrating that the adver-

sarial FPGA tenant could conduct both accuracy degradation attack and targeted attack to hijack DNN function in the victim tenant, under both deep learning white-box and black-box setup. The key contributions of this work are summarized as follows:

- The proposed Adversarial weight duplication (AWD) attack is a novel FPGA hardware-based attacking method, leveraging the co-tenancy of different FPGA users, to aggressively overload the shared power distribution system (PDS) and duplicate certain DNN model weight packages during data transmission between off-chip memory and on-chip buffer.
- To guide AWD attack by identifying the most vulnerable DNN weight data packages for any given malicious objective, we propose a generic vulnerable weight package searching algorithm, called *Progressive Differential Evolution Search (P-DES)*, which is, for the first time, adaptive to both deep learning white-box and black-box setup. Unlike prior works only working in a deep learning white-box setup, such adaptiveness mainly comes from the fact that the proposed P-DES does not require any gradient information of DNN model.
- Comprehensive Deep-Dup attack framework is then developed to integrate both proposed FPGA hardware fault injection scheme (i.e. AWD) and DNN vulnerable parameter searching algorithm (i.e. P-DES) to conduct adversarial weight attack with two different attack objectives (un-targeted attack to degrade overall accuracy and targeted attack to degrade only targeted group accuracy), not only in a traditional Deep Learning (DL) white-box model but also in a DL black-box model with no knowledge of DNN model parameters (e.g., weights, gradients, and architectures).
- A multi-tenant FPGA prototype is developed to validate the proposed Deep-Dup for two different deep learning applications (i.e., Object Detection and Image Classification). Successful un-targeted and targeted attacks are demonstrated in six different popular DNN architectures (e.g. YOLOv2, ResNet-50, MobileNetV2, etc.) on three data sets (e.g., COCO, CIFAR-10, and ImageNet).
- As proof-of-concept, our Deep-Dup black-box attack successfully target the ‘*Ostrich*’ class images (i.e., 100 % attack success rate) on ImageNet with only 26 (out of 23 Million) weight package duplication (i.e. AWD attacks) on ResNet-50 running in FPGA. Besides, Deep-Dup requires just one AWD attack to completely deplete the intelligence of compact architectures (e.g., MobileNetV2).

2 Background

2.1 Related Attacks on Multi-tenant FPGA

The re-programmability of FPGA makes it a popular hardware accelerator for customized computing [31]. To further explore the advantages of FPGA, leading hardware vendors like Intel and Xilinx have integrated FPGAs with CPUs [13] or ARM cores to build flexible System-on-Chips (SoCs) [32, 33]. These heterogeneous computing platforms have recently been integrated into cloud data centers [34], where the hardware resources are leased to different users. The *co-tenancy* of multiple users on the same FPGA chip, although improves the resource utilization efficiency and performance, but also creates a unique attack surface, where many new vulnerabilities will appear and cause dangerous results. With many critical hardware components (e.g., power supply system) being jointly used in the multi-tenant FPGA environment, a malicious tenant can leverage such *indirect* interaction with other tenants to implement various new attacks.

Generally, the attacks on multi-tenant FPGAs can be classified into two classes: 1) side-channel attack, in which the adversarial FPGA user can construct hardware primitive as sensors (e.g., ring oscillator (RO)), to track and analyze the secret of victim user. For example, in [34], the RO-based sensor used as power side-channel has successfully extracted the key of RSA crypto module, similarly, key extraction from advanced encryption standard (AES) is successfully demonstrated in [35] based on RO-caused voltage drop. More recently, it has been demonstrated that a malicious user can leverage the crosstalk between FPGA long-wires as a remote side-channel to steal secret information [36, 37]. 2) Fault injection attack, in which the adversary targets to inject faults to or crash the applications of victim users. For example, the entropy of true random number generator is corrupted by power attacks in multi-tenant FPGAs [38]. In [39], the aggressive power consumption by malicious users causes a voltage drop on the FPGA, which can be leveraged to introduce faults.

With Machine Learning as a service (MLaaS) [40, 41] becoming popular, public lease FPGAs also become an emerging platform for acceleration purposes. However, the security of using multi-tenant FPGA for DNN acceleration is still under-explored in existing works, which is the main target of this paper. Specially, the proposed Deep-Dup methodology belongs to the fault injection category, which leverages malicious power-plundering circuits to compromise the integrity of the DNN model, achieving un-targeted or targeted attack objectives.

2.2 Deep Learning Security

There has been a considerable amount of effort in developing robust and secure DL algorithms [18, 19, 22, 25, 42–49]. Existing deep learning attack vectors under investigation mainly fall into three categories: 1) Attacks that either mislead prediction outcome using maliciously crafted queries (i.e., ad-

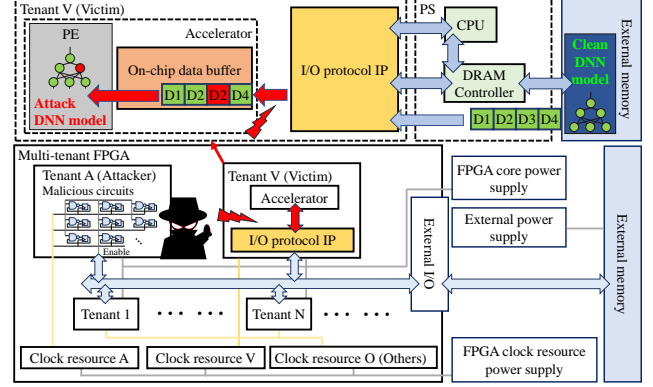


Figure 1: Threat model for the proposed Deep-Dup.

versarial inputs/examples [22, 50]) or through miss-training the model with poisoned training set (i.e., data poisoning attacks [51, 52]). 2) DL information leakage threats such as membership inference attacks [49, 53] and model extraction attacks [47, 54] where adversaries manage to either recover data samples used in training or infer critical DL model parameters. 3) Finally, adversarial fault injection techniques have been leveraged to intentionally trigger weight noise to cause classification errors in a wide range of DL evaluation platform [26–29, 55].

The first two attacks are generally considered as *external adversaries* that exploit training and inference inputs to the deep learning model. Despite the progress in protecting DNN against these external adversaries [21–23], neglecting internal adversarial fault injection still puts the overall security of DNN acceleration in FPGA (DNN-FPGA) systems under threat. The most recent adversarial weight attacks [27, 28, 30, 56] demonstrated, in both deep learning algorithm and real-world general-purpose computer system, that it is possible to modify an extremely small amount (i.e., tens out of millions) of DNN model parameters using row-hammer based bit-flip attack in computer main memory to severely damage or hijack DNN inference function. Even those injected faults might be minor if leveraged by a malicious adversary, such internal *adversarial fault injection* harnessing hardware vulnerabilities may be extremely dangerous as they can severely jeopardize the confidentiality and integrity of DNN system.

3 Threat Model and Attack Vector

Multi-tenant FPGA Hardware Threat Model. In our proposed Deep-Dup, we consider the representative hardware abstraction of multi-tenant FPGA used in the *security* works [36, 57, 58] and *operating system* works [17, 59]. The threat model is shown in Fig. 1, which has the following characteristics: (1) Multiple tenants *co-reside* on a cloud-FPGA and their circuits can be executed simultaneously. The system administrator of cloud service is trusted. (2) Each tenant has the flexibility to program his design in the desired FPGA regions (if not taken by others). (3) All tenants share certain

hardware resources on an FPGA chip, such as the PDS and the communication channels with external memory or I/O. (4) We assume that adversary knows the type of transmitted data (i.e., either DNN model or input data) on the communication channel (e.g., I/O protocol IP) connecting the off-chip memory and on-chip data buffer. Adversarial FPGA tenant can learn such information in different ways: i) Using the side-channel leakage from the communication/data channels on the FPGA, e.g., the cross-talk between FPGA long-wires [36]; ii) Practically, the victim FPGA tenant can be the provider of Machine learning as a service (MLaaS) [40, 41], who offer accelerated DNN computation on multi-tenant FPGA, and the adversary can rent such service as a normal customer, then he/she can learn some info of the model and query outputs.

Deep Learning (DL) Algorithm Threat Model. Regarding Deep Learning (DL) algorithm level threat model, in this work, similar to many other DL security works [18, 21, 26–28, 56, 60], two different DL algorithm threat models are considered and defined here: 1) *DL white-box*: attacker needs to know model architectures, weight values, gradients, several batches of test data, queried outputs. 2) *DL black-box*: attacker only knows the queried outputs and a sample test dataset. Unlike the traditional DL white-box threat model [18, 21, 27, 61], our DL white-box is even weaker with no requirement of computing gradient during the attacking process. Since different DL security works may have different definitions of white/black-box, throughout this work, we will stick to the definition here, which is commonly used in prior works [27, 61, 62]. In this work, similar to many adversarial input or weight attacks, we only target to attack a pre-trained DNN inference model in FPGA, i.e., hijacking the DNN inference behavior through the proposed Deep-Dup, not the training process, which typically requires extra access to the training supply chain [24, 63].

In this threat model shown in Fig. 1, the adversary will conduct our proposed AWD attack on the I/O protocol IPs to duplicate our P-DES searching algorithm identified weight packages into its following neighbor, when transmitting DNN model from off-chip memory to on-chip buffer/processing engine (PE), resulting in a weight perturbed DNN model in the PEs. After attack, the DNN function is hijacked by an adversary with malicious behaviors, such as accuracy degradation or wrong classification of a targeted output class, which will be defined in detail in Sec. 4.

4 Attack Objective Formulation

The proposed Deep-Dup attack is designed to perform both un-targeted and targeted attacks. In this work, we consider two attack objectives: un-targeted and targeted, which are formally defined as below.

Un-targeted Attack. The objective of this attack is to degrade the overall network inference accuracy (i.e., miss-

classifying whole test dataset), thus maximizing the inference loss of DNN. As a consequence, the objective can be formulated as an optimization problem:

$$\max \mathcal{L}_u = \max_{\{\hat{W}\}} \mathbb{E}_{\mathbf{x}} \mathcal{L}(f(\mathbf{x}, \{W\}); \mathbf{t}) \quad (1)$$

where \mathbf{x} and \mathbf{t} are the vectorized input and target output of a given test batch and $\mathcal{L}(\cdot, \cdot)$ calculates the loss between DNN output and target. The objective is to degrade the network’s overall accuracy as low as possible by perturbing weights of the clean DNN model from W to \hat{W} .

Targeted Attack. Different from the un-targeted attack, the objective of targeted attack in this work is to misclassify a specific (target) class of inputs (t_s). This attack objective is formulated in Eq. 2, which can be achieved by maximizing the loss of those target class:

$$\max \mathcal{L}_t = \max_{\{\hat{W}\}} \mathbb{E}_{\mathbf{x}_s} \mathcal{L}(f(\mathbf{x}_s, \{W\}); \mathbf{t}) \quad (2)$$

where \mathbf{x}_s is a sample input batch belongs to the target class t_s .

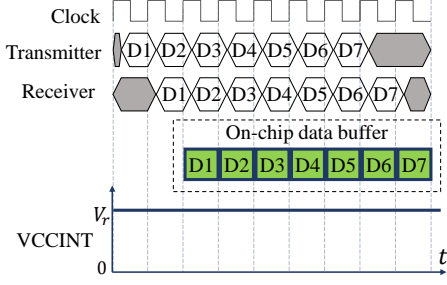
5 Proposed Deep-Dup Framework

Deep-Dup mainly consists of two modules: 1) *adversarial weight duplication (AWD)*, a novel FPGA hardware fault injection scheme leveraging power-plundering circuit to intentionally duplicate certain DNN weight packages during data transmission between off-chip memory and on-chip buffer; 2) *progressive differential evolution search (P-DES)*, a generic searching algorithm to identify most vulnerable DNN weight package index and guide AWD to attack for given malicious objective. We will first describe these two main modules and present Deep-Dup overview framework for both deep learning white-box and black-box attacks at the end of this section.

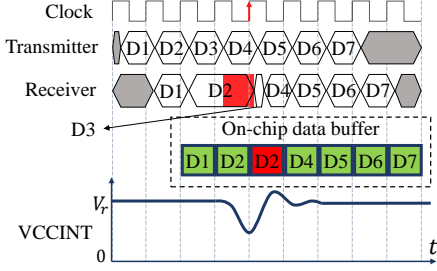
5.1 AWD attack in multi-tenant FPGA

5.1.1 Preliminaries of DNN model implementations

The schematic of an FPGA-based DNN acceleration is illustrated in Fig. 1, which employs various hardware components, including the processing system (PS), processing engine (PE), and external (off-chip) memory. Due to the increasing complexity of modern DNN algorithms, the model size also increases accordingly, which often exceeds the available on-chip resources (e.g., memory). Therefore, the practical DNN computation is usually accomplished in a *layer-by-layer* style, i.e., input data like image and DNN model parameters of different layers are usually loaded and processed separately [64–66]. This solution, although significantly reduces the limits of executing large DNN models in FPGA, also makes real-time data transmission a necessity and sometimes even a bottleneck [67, 68]. Fig. 1 shows the flow of FPGA I/O protocol IP for typical DNN model transmission, in which the on-chip data buffer sends a data transaction request to PS for loading data from external memory. Then, the processing



(a) DNN model transmission w/o attack. Each DNN weight package (D_i) is transmitted and received in a separate clock cycle.



(b) DNN model transmission under AWD attack. Note that the voltage glitch incurs more propagation delay to the transmission of victim package D2, which also shortens the next package D3. As a result, the data package D2 is sampled twice by the receiver clock and duplicated in the on-chip data buffer.

Figure 2: Illustrated timing diagrams of DNN model transmission under different scenarios: w/o or under attack.

engine (PE) will implement computation based on the DNN model in the on-chip data buffer (e.g., BRAM).

The reliable execution of a digital circuit or system on FPGA strictly depends on the relationship between clock and data, i.e., whether they are synchronized at the same pace. A common data transmission schematic is shown in Fig. 2a, in each clock cycle, a *data package* (D_i) is transmitted from transmitter (e.g. external memory) to receiver, such as on-chip data buffer. In the I/O protocol IPs of an FPGA, the data transmission depends on several parameters, like data packaging rules, synchronization control (handshaking) methods, bandwidth, and clock frequency. Taking the advanced eXtensible interface4 (AXI4) as an example [69], all AXI4 communication channels use the same two-way control flow: transmitter and receiver first inform each other whether they are ready for data transaction. In detail, the receiver first sends a data request with an external memory address, and then it will be notified to read the data when it is ready. The size of each transmitted data package depends on the channel bandwidth. Taking DNN model transmission as an example, the normal (w/o attacks) transmission flow with each D_i as a DNN weight package is illustrated in Fig. 2a, with FPGA core voltage (VCCINT) being stable at the recommended supply voltage (V_r), N data packages (e.g., weights) can be transmitted in N clock cycles (D1-D7 in Fig. 2a).

5.1.2 AWD Attack on DNN model

The power supply of modern FPGA chips is regulated based on their voltages, different components will be activated following the order of their nominal voltage, e.g., from low to high [70–72]. Most FPGAs utilize a hierarchical power distribution system (PDS)², which consists of some power regulators providing different supply voltages [71, 72, 74]. A critical component of PDN is capacitors used as the “power bank” for the operational reliability of FPGA. For example, when an FPGA chip’s power supply is suddenly overloaded (i.e., by a transient higher power demand), these capacitors are discharged to compensate for the extra power that regulators cannot immediately provide. The capacitors of the FPGA PDN are usually sized accordingly to fit the practical need. Formally, the default output capacitance (C_{out}) of an FPGA is usually sized to compensate for the current difference for at least two clock cycles with a tolerable voltage drop [74]. As calculated in Eq. 3, where ΔI_{out} and ΔV_{out} represent the changes of the output current and voltage, respectively, and f_{sw} denotes the regulator switching frequency.

$$C_{out} = \frac{2 \times \Delta I_{out}}{f_{sw} \times \Delta V_{out}} \quad (3)$$

As one of FPGA’s most critical parameters, the clock signals provide standard and global timing references for all on-chip operations. In practice, to generate different timing signals, i.e., with different frequencies or phases, FPGAs are equipped with several clock management components, such as the phase-lock-loop. The on-chip clock signals are usually generated by various clock management components, and their reliability is heavily dependent on the robustness of these components. To enhance clock integrity, these clock components are powered by separate supply voltage resources (Fig. 1) from the computing elements like PE. For example, the clock components of Xilinx FPGAs are powered by the auxiliary voltage VCCAUX rather than the FPGA core supply voltage VCCINT [75]. Such a separate power supply mechanism ensures sufficient energy for the operation of these clock components, thus enhancing reliability.

The execution of DNN acceleration in FPGA is significantly relying on the integrity of DNN model. Our proposed AWD attack is motivated by two facts: 1) As aforementioned, the reliability and correctness of FPGA applications are ensured by the power delivery mechanism; 2) based on the power regulation mechanism, there exists a *maximum power capacity* that FPGA PDS can provide to PEs. Thus, if the FPGA PDS is overloaded, FPGA applications might encounter faults caused by the timing violation between clock signal and computation/data. Recent works have demonstrated that the activation of many power-plundering circuits (e.g., ROs), can cause transient voltage drop on the

²PDS is the official terminology of Xilinx FPGAs, which is named as power distribution network in Intel FPGAs [73]. For uniformity, we use PDS in this paper.

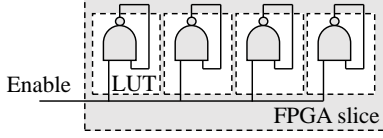


Figure 3: A controllable design scheme that can be leveraged to construct malicious power-plundering circuits on FPGA.

FPGA [35, 38, 76], thus incurring fault injection. Considering the importance of frequent and real-time DNN model transmission from/to FPGA, The basic idea for AWD attack is that a malicious FPGA tenant can introduce a timing violation to the DNN model transmission from off-chip memory to the on-chip data buffer. As illustrated in Fig. 2a, a stable FPGA core voltage (V_{CCINT}) (i.e., with trivial or no fluctuations) will not cause timing violations to data transmission. However, an unstable V_{CCINT} will incur serious timing violations. For example, a sudden voltage drop will make the digital circuit execution slower than usual, causing longer propagation delay to the data transmission. As shown in Fig. 2b, the adversary’s aggressive power plundering creates a voltage drop/glitch that incurs slows down the data transmission channel. As a result, the corresponding data package (e.g., D2) is read twice by the receiver clock, as being duplicated. We envision that the duplicated weight data packages will impact the DNN computation, inducing either significant performance loss, or other malicious/unexpected behaviors.

5.1.3 Power-plundering Circuit

A power-plundering circuit can be achieved with any design scheme that consumes more dynamic power than normal circuit schemes. To make such power-plundering circuit more stealthy, some recent works also employ components of common FPGA applications to cause voltage glitch/drop, e.g., the shift registers of an AES circuit [16] and the XOR tree circuit [77]. Since this work focuses on the security of DNN model in multi-tenant FPGA, thus for simplicity, we adopt an efficient and controllable power-plundering circuit scheme. The design scheme is shown in Fig. 3, which leverages the look-up tables (LUT, the basic FPGA component) in each FPGA slice to build the power-plundering circuit. Slice is another basic FPGA component comprised of 4 look-up tables in most modern FPGAs. In detail, each LUT is instantiated as a NAND gate, and the 4 LUT-based NAND gates of a slice are controlled by an *Enable* signal. An adversarial FPGA tenant can build a large number of such power-plundering cells, which are controlled by the same *Enable* signal. Upon activation, the power-plundering circuit will immediately overload the FPGA PDS and introduce transient voltage drop shown in Fig. 2b, thus implementing AWD attack.

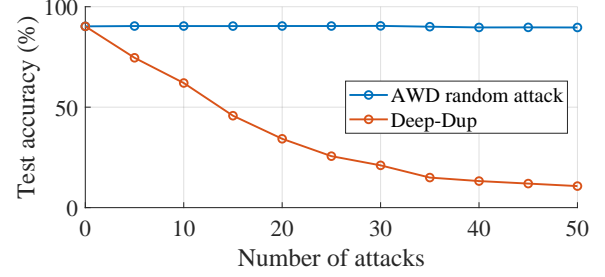


Figure 4: The blue curve shows the validation results of randomly applying 5 to 50 AWD attacks on VGG-11, which does not hamper the test accuracy on CIFAR-10 dataset. The orange curve demonstrates the effectiveness of the proposed Deep-Dup (combining AWD attack with the proposed P-DES searching algorithm), i.e., only 20 attacks is sufficient to degrade the accuracy to below 30 %.

5.1.4 Applying AWD in a Random Way

To validate the effectiveness of AWD attack, we randomly apply it on two different popular DNN models³: VGG-11 [78], an image classification model and YOLOv2 [79], an object detection DNN model. Specifically, the performance of VGG-11 is validated with the CIFAR-10 dataset [80]. The inference accuracy of VGG-11 after applying for different numbers (5 to 50) of AWD attacks is shown as the blue curve in Fig. 4. It can be found that, while being applied in a random manner, the AWD attacks barely degrades the performance of VGG-11. Similarly, we conduct 500 random AWD attack on YOLOv2, and found that the mean Average Precision (mAP⁴) value of YOLOv2 only degrades for $\sim 2\%$ (from 0.428 to 0.419). These experimental results align with the conclusion from many prior DL security works, that a DL model is relatively robust to a random weight noise or perturbation [27, 28]. In other words, even the adversarial FPGA tenant can utilize the proposed AWD to inject fault into DNN model, there still needs an efficient searching method to identify the most vulnerable weight packages to attack for achieving given malicious objective (i.e., un-targeted and targeted attacks). For example, in contrast to the random attack in Fig. 4, our proposed P-DES search algorithm incorporated in Deep-Dup can effectively degrade VGG-11 test accuracy to below 30 % with only 20 attacks (brown curve (Deep-Dup)), where the detailed experimental results will be reported in later section 7. We will present the details of our proposed search algorithm in next subsection.

5.2 Progressive Differential Evolution Search (P-DES) Algorithm

This section delineates the proposed vulnerable weight searching algorithm, called *Progressive Differential Evolution Search (P-DES)*, to generate a set of weight data package

³The detailed experimental setup will be introduced in Sec. 6.1

⁴The important performance metric of YOLOv2 [81].

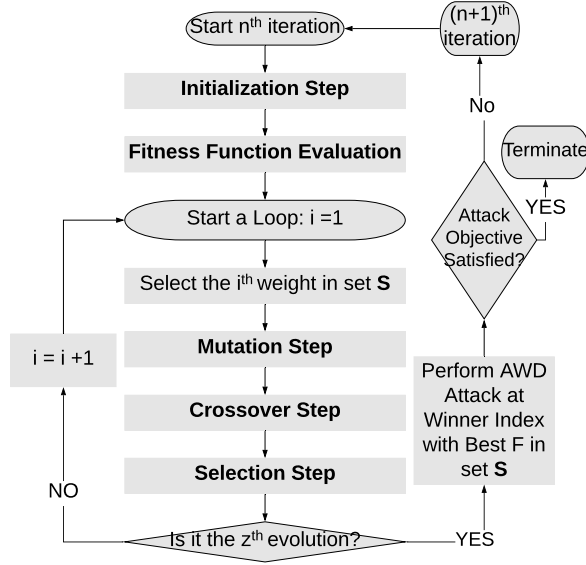


Figure 5: Overview of proposed adversarial weight index searching (P-DES) algorithm.

index for AWD to attack, given attack objective. To formally define the problem, let's first consider a L layer network with weight parameters- $W_{l=1}^L$. Then, the after-attack (i.e. perturbed) weight of the target DNN model executed in FPGA will become $\hat{W}_{l=1}^L$. We model different attack objectives aiming to minimize the difference between $W_{l=1}^L$ and $\hat{W}_{l=1}^L$ for deriving the minimal number of required AWD attacks performing both defined un-targeted and targeted attack objectives.

We will first model the white-box attack, assuming attacker knows the exact model parameters (i.e. weight values and architecture). We assign each weight package in the target DNN with two indexes (p, q) ; where p denotes the layer index and q denotes the index of weight at layer p after flattening the weight matrix W ($W \in R^{m \times n \times a \times kw}$) into a 1D array. Note that, here the weight package refers to one data package that is transmitted in one clock cycle. In the following, we may just call it weight for simplification. The proposed search algorithm is general and applicable for both attack objectives described in Sec. 4. The adaption to black-box attack using P-DES will be discussed at the end of this sub-section.

P-DES is a progressive search algorithm integrating with concept of differential evolution [82–84]. The goal is to progressively search for one weight index at each iteration to guide AWD attack until attacker defined malicious objective is satisfied. The flow chart of proposed P-DES is shown in Fig. 5. For n^{th} iteration, it starts by initializing a set of random weight candidates (i.e. population set - S) for attacker to perform AWD attack and evaluate each attack effect (i.e. fitness function) at current iteration. Then it runs through a succession of evolutionary steps: *mutation*, *crossover* and *selection* for z times (known as number of *evolution*, '500' in this work) to gradually replace original candidates with better ones for achieving the attacker defined malicious objective. When z

times evolution is finished in one search iteration, the attacker picks one best candidate (weight index with highest fitness function value- F) among the final survived population set S and conduct AWD attack on this winner weight location to duplication data package as described in previous sub-section. The detailed description of each step is as follow:

Initialization Step. As shown in Fig. 5, the n^{th} iteration starts by randomly picking an initial weight candidate set that we define as population set S . The population set contains the weight index candidates for guiding attacker to perform AWD attack at current iteration. At the end of current iteration, the attacker will pick one best winner candidate in population set S to perform AWD attack at its index pointed weight data package. The objective of differential evolution is to improve population set S over time to gradually reach attacker defined malicious objective. The S contains z weights whose indexes located at (p_l, q_l) ; where $l = 1, 2, 3, \dots, z$. Here, z is the size of set S , defined as the number of evolution. Ideally, a larger population set (i.e., higher z) would result in a better attack performance at the cost of increased searching time.

Fitness Function Evaluation. Fitness function - F_l is an important step of an evolutionary algorithm to evaluate the attack effect of each proposed candidate in the population set S . In our Deep-Dup attack, as defined in Eq. 1 and Eq. 2, we assign the DNN loss function as fitness function. Thus we could evaluate the attack effect (i.e. F_l) of each candidate in set S in terms of DNN loss. Note that, for white-box attack, such evaluation (i.e. fitness function) could be computed in an off-line replicated model. For black-box attack, loss will be directly evaluated in FPGA by conducting AWD attack in the proposed candidate index pointed data package clock. In next sub-section, a detailed Deep-Dup framework for both white-box and black-box attacks will be discussed. In P-DES, the attacker's goal is to maximize the fitness function - F_l to achieve un-targeted (Eq. 1) or targeted attack (2):

$$F_l \in \{L_u, L_t\} \quad (4)$$

where L_u is un-targeted attack loss and L_t is targeted attack loss. Note that, after each evaluation of F_l , attacker needs to restore the original weight values W by reloading the weights, to guarantee each fitness function is evaluated only based on one corresponding attack weight index.

Mutation Step. For each weight index candidate in population set S , the mutation step generates new candidates using specific mutation strategy to improve current population set. In this work, we integrate four popular mutation strategies [85, 86], where each one generates one mutant vector. Thus, a mutant vector ($\{p_{mut}, q_{mut}\} = \{(p_{mut1}, q_{mut1}); (p_{mut2}, q_{mut2}); (p_{mut3}, q_{mut3}); (p_{mut4}, q_{mut4})\}$) is generated for each weight index candidate:

Strategy 1:

$$p_{mut1} = p_a + \alpha_1(p_b - p_c); \quad (5)$$

$$q_{mut1} = q_a + \alpha_1(q_b - q_c) \quad (6)$$

Strategy 2:

$$p_{mut2} = p_a + \alpha_1 \times (p_b - p_c) + \alpha_2 \times (p_d - p_e); \quad (7)$$

$$q_{mut2} = q_a + \alpha_1 \times (q_b - q_c) + \alpha_2 \times (q_d - q_e) \quad (8)$$

Strategy 3:

$$p_{mut3} = p_a + \alpha_1(p_{best} - p_a) + \alpha_2(p_b - p_c) + \alpha_3(p_d - p_e); \quad (9)$$

$$q_{mut3} = q_a + \alpha_1(q_{best} - q_a) + \alpha_2(q_b - q_c) + \alpha_3(q_d - q_e) \quad (10)$$

Strategy 4:

$$p_{mut4} = p_a + \alpha_1(p_{best} - p_{worst}); \quad (11)$$

$$q_{mut4} = q_a + \alpha_1(q_{best} - q_{worst}) \quad (12)$$

where $\alpha_1, \alpha_2, \alpha_3$ are the mutation factors sampled randomly in the range of $[0,1]$ [85]. a, b, c, d, e are random numbers ($a \neq b \neq c \neq d \neq e$) generated in the range of $[0,z]$. (p_{best}, q_{best}) and (p_{worst}, q_{worst}) are the indexes with the best and worst fitness function values. Note that, both p and q for each layer are normalized to the range of $[0,1]$, which is important since the amount of weights at each layer is different.

Crossover Step. In the crossover step, attacker mixes each mutant vector (p_{mut}, q_{mut}) with current vector (p_i, q_i) to generate a trial vector (p_{trial}, q_{trial}):

$$\text{if } p_{mut} \in [0,1] : p_{trial} = p_{mut}; \quad \text{else} : p_{trial} = p_i \quad (13)$$

$$\text{if } q_{mut} \in [0,1] : q_{trial} = q_{mut}; \quad \text{else} : q_{trial} = q_i \quad (14)$$

The above procedure guarantees attacker only chooses the mutant feature with a valid range of $[0,1]$. Then, the fitness function is evaluated for each trial vector (i.e., $F_{trial1}, F_{trial2}, F_{trial3}, F_{trial4}$). This crossover step ensures attacker can generate a diverse set of candidates to cover most of DNN weight search space.

Selection Step. The selection step selects only the best candidate (i.e. winner with the highest fitness function value) between the trial vector set ($\{p_{trial}, q_{trial}\}$ with four trial vectors) and current candidate (p_i, q_i). Then, the rest four will be eliminated.

Above discussed mutation, crossover and selection will repeat z times to cover all candidates in the population set S . As a result, the initial randomly proposed S will evolve over time to gradually approach attacker defined malicious objective. When z times evolution is finished, the attacker could perform AWD attack at the winner (with highest fitness function value in S) weight index corresponding clock. The P-DES will check if the attack objective has been achieved. If yes, P-DES stops. If not, it goes to next iteration for next round of evolution.

P-DES Adaption to Black-Box Attack. For white-box attack, the P-DES algorithm could work independently exactly the same as we discussed above in an off-line replicated DNN

software model since the attacker already knows all model info. When P-DES is finished, it will directly generate the final weight candidates for AWD to attack in FPGA. However, for a black-box attack, the attacker can only access the input and output scores of the target DNN in victim tenant FPGA, with no knowledge of DNN architecture (i.e., above p refers to # of layers & q refers to # of weights at each layer) information. To adapt above discussed P-DES algorithm to a black-box attack, instead of using architecture info of p and q (i.e., 2D vector), we will treat the whole network parameter to be unwrapped into a 1D vector w , where attacker tries to identify each weight with one feature \hat{p} . Here, \hat{p} denotes the weight index to be attacked after flattening and combining all L layers weights sequentially. As we defined in the threat model section, this is feasible since attacker knows exactly which clock cycles are used to transmit DNN model weights, enabling attacker to develop such 1D weight index vector for P-DES. Thus, two slight modifications in above discussed P-DES algorithm are needed to adapt to black-box attack: 1) 1D \hat{p} mutation vector instead of 2D $\{p, q\}$ mutation vector; 2) fitness function evaluated in FPGA for black-box attack instead of off-line replicated software model in white-box attack. All rest of P-DES algorithm remains the same for both white-box and black-box attacks.

5.3 Deep-Dup: Integrating AWD and P-DES

This section discusses the proposed Deep-Dup attack framework integrating hardware AWD fault injection and software P-DES searching algorithm. In detail, we discuss the feasibility of applying Deep-Dup in both white-box and black-box attack models.

5.3.1 White-Box Attack

As we discussed in the threat model section, white-box attack assumes adversary knows all the details of target DNN model in victim FPGA, including architecture, weight values, gradients, weight package transmission over FPGA I/O protocol IP. For example, such information can be obtained if the victim DNN model is from the most popular ones, such as these from the open-source model zoo [87, 88]. As shown in Fig. 6, knowing these execution details of target DNN model, the adversarial tenant can build an *off-line Deep-Dup simulator* to emulate the behavior of target DNN in victim FPGA. In this off-line simulator, the P-DES algorithm will be used to identify a set of model weight package index transmitted over the I/O protocol IPs, which will guide the attacker to perform AWD attacks on those locations to achieve the defined malicious objective.

5.3.2 Black-Box Attack

As discussed in the threat model in Sec. 3, the victim can be the provider of MLaaS, who uses the multi-tenant FPGA to provide accelerated DNN computation. Therefore, even without full knowledge of DNN model, the adversary can

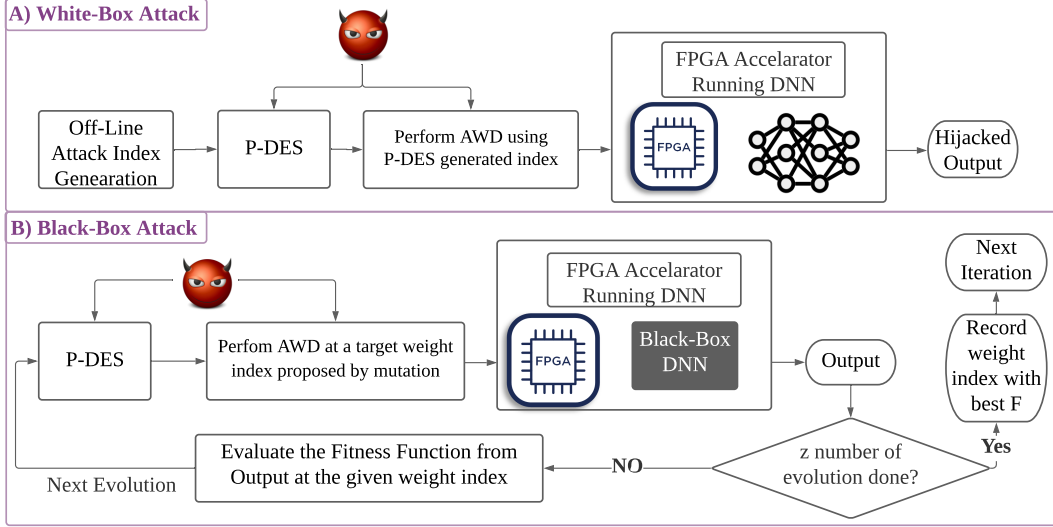


Figure 6: Overview of Deep-Dup attack integrating P-DES and AWD for A) White-Box attack & B) Black-Box Attack.

get access to (i.e., rent) the target DNN model deployed on multi-tenant FPGA, such as feeding inputs and getting the inference output. Moreover, s/he can also leverage an on-chip sensor [89] to collect side-channel leakages from the target multi-tenant FPGA [90] to analyze the DNN weight transmission process. Fig. 6 shows the overview of Deep-Dup black-box attack. Without the off-line Deep-Dup simulator, the proposed Deep-Dup black-box attack utilizes run-time victim DNN in FPGA to evaluate the effectiveness (i.e. fitness function)) of attacking each P-DES mutation proposed weight candidate. Based on the real attack effect in victim DNN inference, P-DES will keep the winner candidate from population set S in each iteration until the pre-defined attack objective is achieved, similar as the P-DES algorithm shown in Fig. 5

6 Experimental Setup

6.1 Dataset and DNN Models

In our experiment, we evaluate three classes of datasets. First, we use CIFAR-10 [80] and ImageNet [3] for image classification tasks. CIFAR-10 is a popular visual recognition dataset, which includes 50 training images and 10k validation set with 32×32 RGB images evenly sampled from 10 categories. The data augmentation technique is identical to previous methods [4]. On the other hand, ImageNet is a large dataset containing 1.2M RGB training images with a size of 224×224 that is divided into 1000 distinct classes. The other application is object detection where we evaluate the attack on the popular COCO [91] dataset. The COCO dataset contains over 200K labeled images in 80 different categories.

For CIFAR-10 dataset, we evaluate the attack against popular ResNet-20 [4] and VGG-11 [78] networks. We use the same pre-trained model with exact configuration as [56, 92]. Then to generate an 8-bit quantized DNN weights using Xilinx Vitis AI [93] model quantization tool [94]. For Im-

ageNet results, we evaluate our attack performance on MobileNetV2 [95], ResNet-18 and ResNet-50 [4] architectures. For MobileNetV2 and ResNet-18, we directly downloaded a pre-trained model from PyTorch Torchvision models⁵ and perform an 8-bit post quantization same as previous attacks [27, 56]. For the ResNet-50, we use Xilinx 8-bit quantized weight trained on ImageNet from [96]. The model we use to validate the YOLOv2 is the official weight [97], trained by COCO [91] dataset, and we quantize [98] each weight value into 16-bits.

6.2 FPGA Configurations

To validate the real-world performance of Deep-Dup, we develop a multi-tenant FPGA prototype, using a ZCU104 FPGA evaluation kit with an ultra-scale plus family MPSoC chip, which has the same FPGA structure as these used in commercial cloud server (e.g., AWS F1 instance), running the above discussed deep learning applications: image classification and object detection. Previous discussed 8-bit quantized DNN models are deployed to our FPGA prototype through high level synthesis (HLS) tool, PYNQ frameworks, and CHaiDNN library from Xilinx [96]. The experimental setup is shown in Fig. 7. For object detection (i.e. YOLOv2) FPGA implementation, multiple types of hardware accelerators (HAs) are used to compute different network layers, such as convolution layer, max-pooling layer, and reorganization layer. Specially, the region layer and data cascade are assigned to the ZYNQ's ARM core. For image recognition (e.g. ResNet-50) FPGA implementation, we follow the same design as Xilinx mapping tool, which only implements the convolution accelerator in a light version (DietChai) [96]. Without loss of generality, the FPGA configurations follow

⁵<https://pytorch.org/docs/stable/torchvision/models.html>

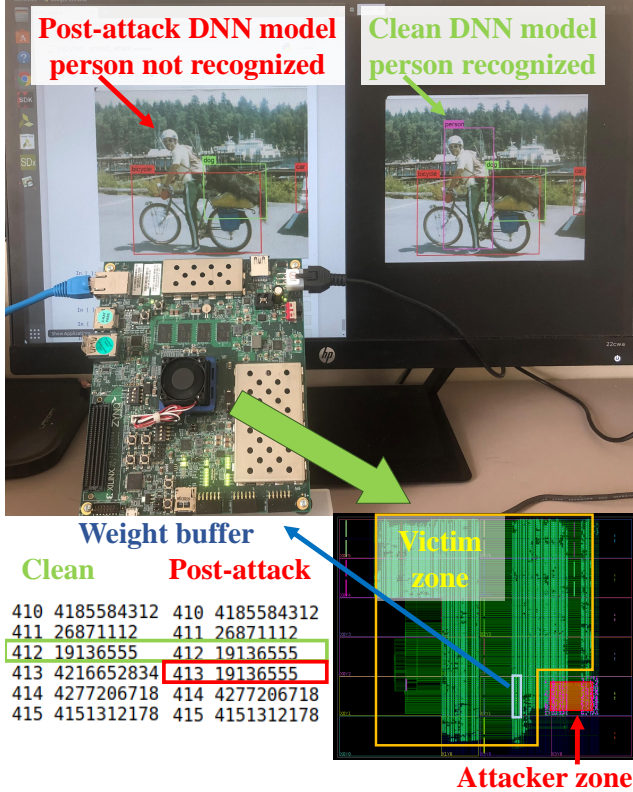


Figure 7: Experimental setup and results of Deep-Dup attack on YOLOv2, with person as target group. DNN weight packages are sampled from the weight buffer to illustrates the effect of AWD attack, which duplicate weight packages with index 412. After attack, the person in the image that can be correctly recognized by the clean YOLOv2 model, however, can not be recognized by the post-attack model.

the official parameters [99] and [96]. Object detection network (i.e. YOLOv2) in FPGA execution frequency is 180MHz. Image recognition DNN network (e.g. ResNet-50) in FPGA execute frequency is 150MHz/300MHz, where the DSP uses a 300MHz clock source to increase the throughput and the rest logic uses a 150MHz clock.

To emulate multi-tenant FPGA environment, we divide the FPGA resources into victim and attacker zones, respectively. The victim zone runs target DNN models, like YOLOv2 or ResNet-50, while the attacker zone mainly consists of malicious power-plundering circuits. Moreover, to limit the available resources of attacker, only 13.38% of the overall FPGA resources are assigned for the power-plundering circuits. During the attacking process, we toggle the Enable signal for the power-plundering circuit to induce AWD attacks, while the victim’s DNN accelerators are loading weight packages from the external memory. As illustrated in Fig. 7, the Deep-Dup attack on DNN model transmission will render the target weight packages received twice by the on-chip data buffer. Therefore, with more AWD attacks being conducted, the actually loaded on-chip DNN model will be more different from the clean

version.

6.3 Attack Evaluation Metric and Hyper-Parameters

For classification application, we use *Test Accuracy (TA)* as the evaluation metric. Test Accuracy is the percentage of samples correctly classified by the network. We denote the test accuracy after the attack as *Post-Attack TA*. For a targeted attack, we use *Attack Success Rate (ASR)* to evaluate the performance of attack; ASR is the percentage of the target class samples miss-classified to an in-correct class after attack. For the object detection application, we use *Mean Average Precision (mAP)* as the evaluation metric that is the primary metric in the official COCO dataset challenge website ⁶.

We also want to report several hyper-parameters of P-DES algorithm of our Deep-Dup attack, which is important for attack efficacy. First, the attack evolution (z) is set to 500 (white-box) and 100 (black-box). In our un-targeted attack, we use a test batch containing 128/25 images for the CIFAR-10/ImageNet dataset. For the targeted attack, we split the target class (t_s) images into two parts: the attacker uses the first set to conduct attack, and the second set is used to evaluate attack success rate. We experimentally tune each hyper-parameter to find the optimum one for each dataset. For an un-targeted attack, we stop P-DES searching whenever the attack achieves near-random guess test accuracy (i.e., $(1/\text{no. of class}) \times 100$ [27]). As for the targeted attack, the attack stopping criteria is to achieve above 99.0 % ASR. For object detection, we stop P-DES searching after degrading the mAP to less than 0.1. Since the evolution search algorithm (P-DES) may converge differently for different rounds, we run three individual rounds of attack and report the median round (in terms of # of Attacks) among them.

7 Experimental Validation and Results

In this section, we first conduct white-box attack on both image classification and object detection. Next, we evaluate the effectiveness of the proposed Deep-Dup attack under a more strict DL-threat model (e.g., Black-Box Attack). Note that, as defined earlier, white-box and black-box attack is just to align with existing prior DL adversarial attack works, referring to how much DNN model information is known to attacker, while the system or hardware threat model is the same. Finally, we present a detailed analysis of the attack through several ablation studies.

7.1 White-Box Attack Results

Image Classification Task. We evaluate the proposed Deep-Dup white-box attack (framework in Fig. 6) on two popular Image Classification dataset in Tab. 1. First, for CIFAR-10, our attack achieves close to the target random guess level accuracy (e.g., 10 % for CIFAR-10) with only 18 model data

⁶<https://cocodataset.org/#detection-eval>

Table 1: Summary of the White-Box Attack on CIFAR-10 and ImageNet Dataset. Here, t_s denotes the target class which we randomly selected for each cases. The number of trainable parameters is reported in M (Million).

| White-Box Attack on Image Recognition | | | | Un-Targeted Attack | | Targeted Attack | | | |
|---------------------------------------|-------------|-----------------|--------|--------------------|--------------|--------------------|-----------------------|---------|--------------|
| Dataset | Network | # of Parameters | TA (%) | Post-Attack TA (%) | # of Attacks | Post-Attack TA (%) | Target Class(t_s) | ASR (%) | # of Attacks |
| CIFAR-10 | ResNet-20 | 0.27 M | 90.77 | 10.69 | 18 | 50.91 | Cat | 99.98 | 13 |
| | VGG-11 | 132 M | 90.74 | 10.72 | 51 | 14.29 | Horse | 99.97 | 86 |
| | MobileNetV2 | 2.1 M | 70.79 | 0.192 | 1 | 8.926 | Lesser Panda | 100.0 | 1 |
| ImageNet | ReNet-18 | 11 M | 69.35 | 0.18 | 106 | 34.45 | Ostrich | 100.0 | 13 |
| | ReNet-50 | 23 M | 72.97 | 0.18 | 180 | 29.59 | Ostrich | 100.0 | 25 |

package duplication through AWD attack (un-targeted) on ResNet-20. However, to deteriorate the test accuracy of VGG-11 to 10.92 % from 90.74 %, Deep-Dup requires 51 AWD attacks. Clearly, VGG-11 is more robust to Deep-Dup attack; the reason might be VGG-11 model is denser (i.e., (132 Million Parameters)) than ResNet-20 (0.27 Million Parameters), as model *density* plays a critical role in enhancing DNN robustness. This observation is consistent with the conclusion of previous adversarial input [21] and weight [28, 92] attacks regarding the co-relation between model density and robustness. Similarly, for targeted attack on CIFAR-10, the attacker requires only 13 and 86 AWD attacks to achieve higher than 99.0 % ASR on ResNet-20 and VGG-11 respectively. Since ResNet-20 requires only 13 attacks to deplete the 'Cat' class accuracy, the overall accuracy of the network remains higher (50.9 %) than the VGG-11 (14.29 %) counterpart.

For ImageNet classification task, Our attack succeeds in degrading MobileNetV2 test accuracy to 0.19 % from 70.79 % with just one *single* AWD attack. Even for the targeted attack, it only requires one AWD attack to achieve 100 % ASR in miss-classifying all *Lesser Panda* images. Again, MobileNetV2 is also found to be extremely vulnerable by previous adversarial weight attack [28] as only a single bit memory error can cause catastrophic output performance. Nevertheless, MobileNet is an efficient and compact architecture ideal for mobile and edge computing platforms like FPGA [100]. Thus the vulnerability of these compact architectures against Deep-Dup raises a fair question of how secure are these DNN models in cloud FPGA? The answer from our Deep-Dup attack is a *big NO*. As for the ResNet family (e.g., 18/50) of architecture, Deep-Dup successfully (i.e., 100 % ASR) attacks class *Ostrich* images with less than 30 attacks. But to perform the un-targeted attack, Deep-Dup runs more than 100 iterations to degrade the accuracy below 0.2% for both ResNet-18 and ResNet-50. Again, for ImageNet, larger DNN models (e.g., ResNet-18 & ResNet-50) shows better resistance to Deep-Dup attack.

Object Detection Task. In the object detection task, YOLOv2 architecture has a baseline Mean Average Precision (mAP) of 0.42 for all the 80 classes. Our attack can degrade the mAP to 0.04 with only 20 AWD attacks. Moreover, Deep-

Table 2: White-Box attack summary on YOLOv2 architecture. We report the mAP both before and after the attack on the COCO dataset. For the targeted attack, we only report the Average Precision (AP) of the corresponding target class.

| White-Box Un-Targeted Attack on YOLOv2 | | | |
|--|--------|------------------|--------------|
| Target Class (t_s) | mAP | Post- Attack mAP | # of Attacks |
| All | 0.428 | 0.04 | 20 |
| White-Box Targeted Attack on YOLOv2 | | | |
| Target Class (t_s) | AP | Post-Attack AP | # of Attacks |
| Person | 0.6039 | 0.07 | 20 |
| Car | 0.5108 | 0.05 | 12 |
| Bowl | 0.329 | 0.01 | 10 |
| Sandwich | 0.4063 | 0.07 | 5 |

Dup can attack a specific class of objects to deteriorate the Average Precision (AP) of only one target object. For example, Deep-Dup can degrade the AP of class *car* from an initial value of 0.5108 to 0.05 after only *twelve* AWD attacks. More examples of targeted attack on the COCO dataset classes are summarized in Tab. 4.

7.2 Black-Box Attack Results

The aforementioned experimental results demonstrate that the proposed P-DES searching algorithm can guide AWD attack in white-box scenario. For proof of concept of the proposed Deep-Dup black-box framework shown in Fig. 6, in this section, we demonstrate the black-box attack on Resnet-50 for image classification task and YOLOv2 for object detection task. Specially, in our case study, we randomly pick "ostrich" class in Imagnet dataset as target class for ResNet-50 and 4 target objects (i.e. Person, Car, Bowl and Sandwich) in COCO dataset for YOLOv2. Other settings and performance metrics are the same as described in Sec. 7.1. The Deep-Dup black-box attack on ResNet-50 are successful and results are reported in Tab. 3. It can be seen that only 26 AWD attacks are needed to attack the "ostrich" with 100 % ASR. Similarly, Deep-Dup black-box attack on YOLOv2 is also successful, as reported in Tab. 4. It can be seen that the post-attack AP is significantly degraded after less than 20 AWD attacks. For

Table 3: Black-Box targeted attack on ResNet-50 architecture pre-trained with ImageNet.

| Black-Box Targeted Attack on ResNet-50 | | | | |
|--|-------|-------------------|---------|--------------|
| (t_s) | TA(%) | Post-Attack TA(%) | ASR (%) | # of Attacks |
| Ostrich | 72.97 | 46.96 | 100 | 26 |

Table 4: Black-Box attack on YOLOv2 architecture. For the targeted attack we only report the AP of the corresponding target class after attack.

| Black-Box Un-Targeted Attack on YOLOv2 | | | |
|--|--------|------------------|--------------|
| Target Class (t_s) | mAP | Post- Attack mAP | # of Attacks |
| All | 0.428 | 0.06 | 30 |
| Black-Box Targeted Attack on YOLOv2 | | | |
| Target Class (t_s) | AP | Post-Attack AP | # of Attacks |
| Person | 0.6039 | 0.0507 | 20 |
| Car | 0.5108 | 0.0621 | 18 |
| Bowl | 0.3290 | 0.0348 | 15 |
| Sandwich | 0.4063 | 0.0125 | 6 |

example, only 6 AWD attacks are needed to decrease the average precision (AP) of sandwich class from 0.4063 to 0.0125.

7.3 Comparison to Other Methods

Previously, very few adversarial weight attack works have been successful in attacking DNN model parameters to cause complete malfunction at the output [26, 29]. Thus we only compare with the most recent and successful adversarial bit-flip (BFA) based weight attack [27, 28], which uses a gradient-based search algorithm to degrade DNN performance in a white-box setting. We also compare our search algorithm (P-DES) to a random AWD attack.

Table 5: Comparison of Deep-Dup with *random* AWD attack and row-hammer based (BFA [27, 28]) attack. All the results are presented for 8-bit quantized VGG-11 model [27].

| Method | Threat Model | TA (%) | Post-Attack TA (%) | # of Attacks |
|-------------------|-----------------------|--------|--------------------|--------------|
| Random | Black Box | 90.23 | 90.07 | 50 |
| BFA [28] | White Box | 90.23 | 10.8 | 28 |
| Proposed Deep-Dup | Black Box & White Box | 90.23 | 10.92 | 50 |

As shown in both Tab. 5 and Fig. 4, only 50 AWD attack iterations can degrade the accuracy of VGG-11 to 10.92 % while randomly performing 50 AWD attacks, can not even degrade the model accuracy beyond 90 %. On the other hand, a BFA attack [28] using row-hammer based memory fault injection technique, requires only 28 attacks (i.e. memory bit-flips) to achieve the same un-targeted attack success (i.e., ~ 10 % TA). However, it could only works in white-box setting, not black-box.

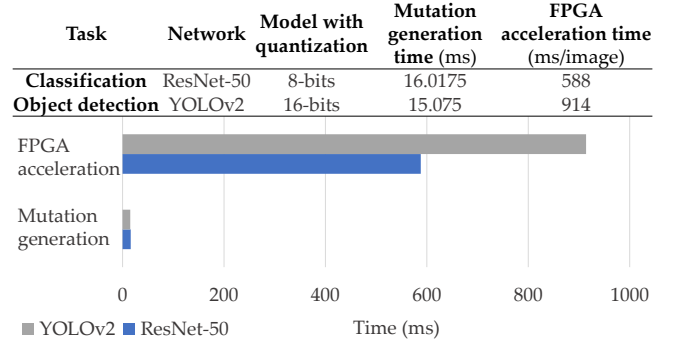


Figure 8: Black-Box attack performance. We compare the FPGA acceleration time with the mutation generation time for one image. Specifically, there are four mutation strategies included in our P-DES algorithm, the complexity of the strategy determine its corresponding generation time, here we only report their average generation time.

7.4 Ablation Study

Attack Time Cost Analysis. Attack time is an important parameter to evaluate the performance of proposed Deep-Dup framework. The execution time of one searching iteration of our proposed P-DES algorithm is constant given a fixed z , regardless of DNN model size. The overall searching time is proportional to the number of evolution (z). For Deep-Dup white-box attack, the P-DES algorithm is executed off-line, and the AWD attack is only executed when the vulnerable weight indexes are generated. Moreover, it should be noted that the hardware AWD attack incurs no time cost, as it runs in parallel with the victim DNN model. For Deep-Dup black-box attack framework shown in Fig. 6, two main time cost includes mutation generation (proportional to z) and FPGA fitness function evaluation (proportional to DNN acceleration latency in FPGA). In Fig. 8, we report the average time cost of the proposed 4 mutation strategies executed in the PS of our FPGA prototype. Additionally, we also report the DNN execution time in FPGA, which is determined by the corresponding DNN model size, architecture, optimization method, and available FPGA hardware resources. It is easy to observe that our P-DES mutation generation only consumes trivial time compared to DNN execution time in FPGA, which is the bottleneck in black-box attack.

Effect of Attack Evolution (z). Our proposed Deep-Dup attack leverages the searching algorithm P-DES to identify vulnerable weight index. The P-DES algorithm at each iteration performs a pre-defined amount of evolution (z) to gradually enhance the initial population set (S) to maximize fitness function (i.e. DNN overall loss or target group loss). Ideally, increasing the value of z should improve the performance of the algorithm, but at the expense of increased searching time. Considering the white-box attack scenario shown in Fig. 6, the P-DES searching runs off-line independent of AWD attack on FPGA, which offers more flexibility to tune value of z . To verify the effect of tuning value of z , we conduct an

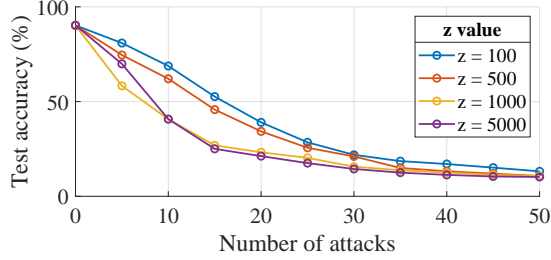


Figure 9: Test accuracy vs Number of attacks plot shows the effect of choosing different values of evolution (z). The four different plots indicate the values of $z = 100/500/1000/5000$ for un-targeted attack on VGG-11 network. For each case we run the attack for 50 times.

Table 6: We show the effect of using each mutation strategy individually and combining all four. The mutation success is the number of times a new trial vector replaces a current population candidate in set S out of 100 evolution. The result is reported as average of five rounds (rounded to nearest integer).

| Mutation Strategy | Mutation Success (%) |
|---------------------|----------------------|
| Strategy-1 | 77 |
| Strategy-2 | 79 |
| Strategy-3 | 80 |
| Strategy-4 | 80 |
| Combination of Four | 86 |

ablation study and results are shown in Fig. 9, where four different plots indicate the attack efficacy by tuning z from 100/500/1000/5000. It demonstrates that even though searching with larger z evolution has a higher initial slope, but they converge in a similar pattern around the 50th iteration. Thus, in this work, we chose a moderate evolution number (z) of 500 for white-box attack and 100 for black-box.

Effect of the Mutation Strategies. Another important component of our P-DES algorithm is the choice of mutation strategy. As we described in P-DES algorithm section, we apply a combined four different strategies to generate one mutant vector each. To see its effect on attack efficacy, we perform another ablation study on different mutation strategies in our proposed P-DES algorithm. Tab. 6 shows the effect of each mutation strategy using a case study where we only attack the ResNet-20 model with just one AWD iteration. We set evolution $z = 100$ and record how many times a new trial vector replaces a candidate in the initial population set S . First, the result indicates all the mutation strategy is working individually, and each achieving a higher than 70 % success rate. Second, a trial vector set generated by the combination of four strategies replaces an initial candidate in the population set 86 times out of 100 evolution. Thus, we conclude that combined mutation strategies are effectively working in improving the initial population set towards achieving the malicious goal.

8 Potential Defense Directions

DNN algorithm-level potential defense directions. Our evaluation of Deep-Dup attack in the previous section demonstrates an obvious co-relation between network capacity (i.e., # of model parameters) and attack resistance (# of attack iterations). In Tab. 1, the ImageNet dataset section depicts, as the size of the network increases from MobileNetV2 to ResNet-50; the number of attacks required to gain 100 % ASR increases as well. We observe the same trend for CIFAR-10 models where VGG-11 (i.e., dense model) requires a higher number of attacks than ResNet-20 (i.e., compact model). As a result, one possible direction to improve DNN model’s resistance to the Deep-Dup attack is to use a dense model with larger learning capacity. Another potential direction could leverage the popular adversarial training concept in defending adversarial input attacks [21]. In adversarial training, the defender trains the DNN to minimize a mixture of two losses: clean (i.e., No-attack) loss and adversarial loss (i.e., from attacked image/weights). Similarly, in the context of the Deep-Dup attack, adversarial training can be formulated to optimize DNN model parameters on two losses: one traditional DNN loss and another computed from the perturbed weight \hat{W} generated by Deep-Dup attack at each iteration. But weight duplication is an in-place operation during training and may break the gradient chain. Thus to implement adversarial training for the Deep-Dup attack in practice requires further investigations.

FPGA System-oriented Defense. In addition to DNN algorithm-level defense, we also envision that the proposed Deep-Dup attack might be mitigated with FPGA system-oriented methods. Since the proposed attack scheme heavily depends on the transmission order of DNN weight packages, i.e., duplicating critical packages to their neighbors. We envision that a potential defense method is to obfuscate the order of DNN model packages, i.e., transmitting the DNN model packages in a random order, or inserting random dummy model package to the DNN model. Therefore, even if the index information of critical DNN weight packages can be identified by the P-DES algorithm, such information cannot be used to attack DNN model in the future. This model obfuscation method can potentially mitigate Deep-Dup attack, but it will also increase the workload of FPGA I/O protocol IPs, i.e., including more dummy packages.

9 Conclusion

In this work, we study the security of DNN acceleration in multi-tenant FPGA. For the first time, we exploit this novel attack surface where victim and attacker share the same FPGA hardware sources. Our proposed Deep-Dup attack framework is validated with a multi-tenant FPGA prototype, as well as some popular DNN architectures (e.g. YOLOv2, ResNet-50, MobileNetV2, etc.) and datasets (e.g., COCO, CIFAR-10, and ImageNet). The experimental results demonstrate that the proposed attack framework can completely deplete DNN inference performance to as low as random guess or attack a specific target class of inputs. It is worth to mention that

our attack succeeds even after assuming the attacker has no knowledge about the DNN inference running in FPGA, yet black-box attack. A malicious tenant with such limited knowledge can implement both targeted and un-targeted malicious objectives to cause havoc for a victim user. Finally, we envision that the proposed attack and defense methodologies will bring more awareness to the security of deep learning application running in modern hardware accelerators.

References

- [1] Yann LeCun and Yoshua Bengio. Convolutional networks for images, speech, and time series. *The handbook of brain theory and neural networks*, 3361(10):1995, 1995.
- [2] Jia Deng, Wei Dong, Richard Socher, Li-Jia Li, Kai Li, and Li Fei-Fei. Imagenet: A large-scale hierarchical image database. In *IEEE Conference on Computer Vision and Pattern Recognition*, pages 248–255. IEEE, 2009.
- [3] Alex Krizhevsky, Ilya Sutskever, and Geoffrey E Hinton. Imagenet classification with deep convolutional neural networks. In *Advances in neural information processing systems*, pages 1097–1105, 2012.
- [4] Kaiming He, Xiangyu Zhang, Shaoqing Ren, and Jian Sun. Deep residual learning for image recognition. In *Proceedings of the IEEE conference on computer vision and pattern recognition*, pages 770–778, 2016.
- [5] Geoffrey Hinton, Li Deng, Dong Yu, George E Dahl, Abdel-rahman Mohamed, Navdeep Jaitly, Andrew Senior, Vincent Vanhoucke, Patrick Nguyen, and Tara N Sainath. Deep neural networks for acoustic modeling in speech recognition: The shared views of four research groups. *IEEE Signal Processing Magazine*, 29(6):82–97, 2012.
- [6] Yann LeCun, Yoshua Bengio, and Geoffrey Hinton. Deep learning. *nature*, 521(7553):436, 2015.
- [7] Wayne Xiong, Jasha Droppo, Xuedong Huang, Frank Seide, Mike Seltzer, Andreas Stolcke, Dong Yu, and Geoffrey Zweig. Achieving human parity in conversational speech recognition. *arXiv preprint arXiv:1610.05256*, 2016.
- [8] B. Shickel, P. J. Tighe, A. Bihorac, and P. Rashidi. Deep ehr: A survey of recent advances in deep learning techniques for electronic health record (ehr) analysis. *IEEE Journal of Biomedical and Health Informatics*, 22(5):1589–1604, Sep. 2018.
- [9] Zhenlong Yuan, Yongqiang Lu, Zhaoguo Wang, and Yibo Xue. Droid-sec: Deep learning in android malware detection. In *Proceedings of the 2014 ACM Conference on SIGCOMM*, SIGCOMM ’14, pages 371–372. ACM, 2014.
- [10] Chenyi Chen, Ari Seff, Alain Kornhauser, and Jianxiong Xiao. Deepdriving: Learning affordance for direct perception in autonomous driving. In *Computer Vision (ICCV), 2015 IEEE International Conference on*, pages 2722–2730. IEEE, 2015.
- [11] M. Teichmann, M. Weber, M. Zöllner, R. Cipolla, and R. Urtasun. Multinet: Real-time joint semantic reasoning for autonomous driving. In *2018 IEEE Intelligent Vehicles Symposium (IV)*, pages 1013–1020, June 2018.
- [12] Altera and ibm unveil fpga-accelerated power systems. <https://www.hpcwire.com/off-the-wire/altera-ibm-unveil-fpga-accelerated-power-systems/>.
- [13] Here’s what an intel broadwell xeon with a built-in fpga looks like, 2016. https://www.theregister.co.uk/2016/03/14/intel_xeon_fpga/.
- [14] Inside the microsoft fpga-based configurable cloud, 2017. <https://azure.microsoft.com/en-us/resources/videos/build-2017-inside-the-microsoft-fpga-based-configurable-cloud/>.
- [15] Enable faster fpga accelerator development and deployment in the cloud, 2020. <https://aws.amazon.com/ec2/instance-types/f1/>.
- [16] George Provelengios, Daniel Holcomb, and Russell Tessier. Power wasting circuits for cloud fpga attacks. In *30th International Conference on Field Programmable Logic and Applications (FPL)*, 2020.
- [17] Yue Zha and Jing Li. Virtualizing fpgas in the cloud. In *Proceedings of the Twenty-Fifth International Conference on Architectural Support for Programming Languages and Operating Systems*, pages 845–858, 2020.
- [18] Ian J Goodfellow, Jonathon Shlens, and Christian Szegedy. Explaining and harnessing adversarial examples. *arXiv preprint arXiv:1412.6572*, 2014.
- [19] Aleksander Madry, Aleksandar Makelov, Ludwig Schmidt, Dimitris Tsipras, and Adrian Vladu. Towards deep learning models resistant to adversarial attacks. *arXiv preprint arXiv:1706.06083*, 2017.
- [20] Christian Szegedy, Wojciech Zaremba, Ilya Sutskever, Joan Bruna, Dumitru Erhan, Ian Goodfellow, and Rob Fergus. Intriguing properties of neural networks. *arXiv preprint arXiv:1312.6199*, 2013.

- [21] Aleksander Madry, Aleksandar Makelov, Ludwig Schmidt, Dimitris Tsipras, and Adrian Vladu. Towards deep learning models resistant to adversarial attacks. In *International Conference on Learning Representations*, 2018.
- [22] Nicholas Carlini and David Wagner. Towards evaluating the robustness of neural networks. In *2017 IEEE Symposium on Security and Privacy (SP)*, pages 39–57. IEEE, 2017.
- [23] Anish Athalye, Nicholas Carlini, and David Wagner. Obfuscated gradients give a false sense of security: Circumventing defenses to adversarial examples. *arXiv preprint arXiv:1802.00420*, 2018.
- [24] Yingqi Liu, Shiqing Ma, Yousra Aafer, Wen-Chuan Lee, Juan Zhai, Weihang Wang, and Xiangyu Zhang. Trojaning attack on neural networks. In *25th Annual Network and Distributed System Security Symposium, NDSS 2018, San Diego, California, USA, February 18–22, 2018*. The Internet Society, 2018.
- [25] Tianyu Gu, Brendan Dolan-Gavitt, and Siddharth Garg. Badnets: Identifying vulnerabilities in the machine learning model supply chain. *arXiv preprint arXiv:1708.06733*, 2017.
- [26] Sanghyun Hong, Pietro Frigo, Yiğitcan Kaya, Cristiano Giuffrida, and Tudor Dumitraş. Terminal brain damage: Exposing the graceless degradation in deep neural networks under hardware fault attacks. In *28th {USENIX} Security Symposium ({USENIX} Security 19)*, pages 497–514, 2019.
- [27] Adnan Siraj Rakin, Zhezhi He, and Deliang Fan. Bit-flip attack: Crushing neural network with progressive bit search. In *The IEEE International Conference on Computer Vision (ICCV)*, October 2019.
- [28] Fan Yao, Adnan Rakin, and Deliang Fan. Deephammer: Depleting the intelligence of deep neural networksthrough targeted chain of bit flips. In *29th {USENIX} Security Symposium ({USENIX} Security 20)*, 2020.
- [29] Yannan Liu, Lingxiao Wei, Bo Luo, and Qiang Xu. Fault injection attack on deep neural network. In *2017 IEEE/ACM International Conference on Computer-Aided Design (ICCAD)*, pages 131–138. IEEE, 2017.
- [30] Adnan Siraj Rakin, Zhezhi He, Jingtao Li, Fan Yao, Chaitali Chakrabarti, and Deliang Fan. T-bfa: Targeted bit-flip adversarial weight attack. *arXiv preprint arXiv:2007.12336*, 2020.
- [31] Jason Cong, Zhenman Fang, Muhuan Huang, Peng Wei, Di Wu, and Cody Hao Yu. Customizable computing—from single chip to datacenters. *Proceedings of the IEEE*, 107(1):185–203, 2018.
- [32] Xilinx: Socs, mpsocs and rfsocs, 2020. <https://www.xilinx.com/products/silicon-devices/soc.html>.
- [33] Intel: Soc fpgas, 2020. <https://www.intel.com/content/www/us/en/products/programmable/soc.html>.
- [34] Mark Zhao and G Edward Suh. Fpga-based remote power side-channel attacks. In *2018 IEEE Symposium on Security and Privacy (SP)*, pages 229–244. IEEE, 2018.
- [35] Jonas Krautter, Dennis RE Gnad, and Mehdi B Tahoori. Fpgahammer: remote voltage fault attacks on shared fpgas, suitable for dfa on aes. *IACR Transactions on Cryptographic Hardware and Embedded Systems*, pages 44–68, 2018.
- [36] Ilias Giechaskiel, Kasper B Rasmussen, and Ken Eguro. Leaky wires: Information leakage and covert communication between fpga long wires. In *Proceedings of the 2018 on Asia Conference on Computer and Communications Security*, pages 15–27. ACM, 2018.
- [37] Yukui Luo and Xiaolin Xu. Hill: A hardware isolation framework against information leakage on multi-tenant fpga long-wires. In *2019 International Conference on Field-Programmable Technology (ICFPT)*, pages 331–334. IEEE, 2019.
- [38] Dina Mahmoud and Mirjana Stojilović. Timing violation induced faults in multi-tenant fpgas. In *2019 Design, Automation & Test in Europe Conference & Exhibition (DATE)*, pages 1745–1750. IEEE, 2019.
- [39] George Provelengios, Chethan Ramesh, Shivukumar B Patil, Ken Eguro, Russell Tessier, and Daniel Holcomb. Characterization of long wire data leakage in deep submicron fpgas. In *Proceedings of the 2019 ACM/SIGDA International Symposium on Field-Programmable Gate Arrays*, pages 292–297. ACM, 2019.
- [40] Machine learning on aws, 2020. https://aws.amazon.com/machine-learning/?nc1=h_ls.
- [41] Cloud automl, 2020. <https://cloud.google.com/automl>.
- [42] Luis Muñoz-González, Battista Biggio, Ambra Demontis, Andrea Paudice, Vasin Wongrassamee, Emil C. Lupu, and Fabio Roli. Towards poisoning of deep learning algorithms with back-gradient optimization. *CoRR*, 2017.
- [43] Andrew Ilyas, Logan Engstrom, Anish Athalye, and Jessy Lin. Black-box adversarial attacks with limited

- queries and information. In *Proceedings of International Conference on Machine Learning, ICML 2018*, July 2018.
- [44] Ekin D Cubuk, Barret Zoph, Samuel S Schoenholz, and Quoc V Le. Intriguing properties of adversarial examples. *ICLR workshop*, 2018.
- [45] Giuseppe Ateniese, Luigi V. Mancini, Angelo Spognardi, Antonio Villani, Domenico Vitali, and Giovanni Felici. Hacking smart machines with smarter ones: How to extract meaningful data from machine learning classifiers. *Int. J. Secur. Netw.*, 10(3):137–150, September 2015.
- [46] Florian Tramèr, Fan Zhang, Ari Juels, Michael K. Reiter, and Thomas Ristenpart. Stealing machine learning models via prediction apis. In *Proceedings of the 25th USENIX Conference on Security Symposium, SEC’16*, pages 601–618. USENIX Association, 2016.
- [47] Nicolas Papernot, Patrick McDaniel, Ian Goodfellow, Somesh Jha, Z. Berkay Celik, and Ananthram Swami. Practical black-box attacks against machine learning. In *Proceedings of the 2017 ACM on Asia Conference on Computer and Communications Security, ASIA CCS ’17*, pages 506–519. ACM, 2017.
- [48] Matt Fredrikson, Somesh Jha, and Thomas Ristenpart. Model inversion attacks that exploit confidence information and basic countermeasures. In *Proceedings of the 22Nd ACM SIGSAC Conference on Computer and Communications Security, CCS ’15*, pages 1322–1333. ACM, 2015.
- [49] Matthew Fredrikson, Eric Lantz, Somesh Jha, Simon Lin, David Page, and Thomas Ristenpart. Privacy in pharmacogenetics: An end-to-end case study of personalized warfarin dosing. In *USENIX Security Symposium*, pages 17–32, 2014.
- [50] Nina Narodytska and Shiva Prasad Kasiviswanathan. Simple black-box adversarial perturbations for deep networks. *arXiv preprint arXiv:1612.06299*, 2016.
- [51] Battista Biggio, Luca Didaci, Giorgio Fumera, and Fabio Roli. Poisoning attacks to compromise face templates. In *Biometrics (ICB), 2013 International Conference on*, pages 1–7. IEEE, 2013.
- [52] Huang Xiao, Battista Biggio, Gavin Brown, Giorgio Fumera, Claudia Eckert, and Fabio Roli. Is feature selection secure against training data poisoning? In *International Conference on Machine Learning*, pages 1689–1698, 2015.
- [53] R. Shokri, M. Stronati, C. Song, and V. Shmatikov. Membership inference attacks against machine learning models. In *2017 IEEE Symposium on Security and Privacy*, pages 3–18, May 2017.
- [54] Manish Kesarwani, Bhaskar Mukhoty, Vijay Arya, and Sameep Mehta. Model extraction warning in mlaas paradigm. In *Proceedings of the 34th Annual Computer Security Applications Conference*, pages 371–380. ACM, 2018.
- [55] Jakub Breier, Xiaolu Hou, Dirmanto Jap, Lei Ma, Shivam Bhasin, and Yang Liu. Deeplaser: Practical fault attack on deep neural networks. *arXiv preprint arXiv:1806.05859*, 2018.
- [56] Adnan Siraj Rakin, Zhezhi He, and Deliang Fan. Tbt: Targeted neural network attack with bit trojan. In *Proceedings of the IEEE/CVF Conference on Computer Vision and Pattern Recognition (CVPR)*, pages 13198–13207, 2020.
- [57] Chethan Ramesh, Shivukumar B Patil, Siva Nishok Dhanuskodi, George Provelengios, Sébastien Pillement, Daniel Holcomb, and Russell Tessier. Fpga side channel attacks without physical access. In *2018 IEEE 26th Annual International Symposium on Field-Programmable Custom Computing Machines (FCCM)*, pages 45–52. IEEE, 2018.
- [58] Sadegh Yazdanshenas and Vaughn Betz. The costs of confidentiality in virtualized fpgas. *IEEE Transactions on Very Large Scale Integration (VLSI) Systems*, 2019.
- [59] Ahmed Khawaja, Joshua Landgraf, Rohith Prakash, Michael Wei, Eric Schkufza, and Christopher J Rossbach. Sharing, protection, and compatibility for reconfigurable fabric with amorpos. In *13th {USENIX} Symposium on Operating Systems Design and Implementation ({OSDI} 18)*, pages 107–127, 2018.
- [60] Zhezhi He, Adnan Siraj Rakin, and Deliang Fan. Parametric noise injection: Trainable randomness to improve deep neural network robustness against adversarial attack. In *Proceedings of the IEEE Conference on Computer Vision and Pattern Recognition*, pages 588–597, 2019.
- [61] Jacob Buckman, Aurko Roy, Colin Raffel, and Ian Goodfellow. Thermometer encoding: One hot way to resist adversarial examples. In *International Conference on Learning Representations*, 2018.
- [62] Pin-Yu Chen, Huan Zhang, Yash Sharma, Jinfeng Yi, and Cho-Jui Hsieh. Zoo: Zeroth order optimization based black-box attacks to deep neural networks without training substitute models. In *Proceedings of the*

10th ACM Workshop on Artificial Intelligence and Security, pages 15–26. ACM, 2017.

- [63] Tianyu Gu, Brendan Dolan-Gavitt, and Siddharth Garg. Badnets: Identifying vulnerabilities in the machine learning model supply chain. *CoRR*, abs/1708.06733, 2017.
- [64] Chen Zhang, Peng Li, Guangyu Sun, Yijin Guan, Bingjun Xiao, and Jason Cong. Optimizing fpga-based accelerator design for deep convolutional neural networks. In *Proceedings of the 2015 ACM/SIGDA International Symposium on Field-Programmable Gate Arrays*, pages 161–170. ACM, 2015.
- [65] Xiaofan Zhang, Hanchen Ye, Junsong Wang, Yonghua Lin, Jinjun Xiong, Wen-mei Hwu, and Deming Chen. Dnnexplorer: A framework for modeling and exploring a novel paradigm of fpga-based dnn accelerator. *arXiv preprint arXiv:2008.12745*, 2020.
- [66] Pengfei Xu, Xiaofan Zhang, Cong Hao, Yang Zhao, Yongan Zhang, Yue Wang, Chaojian Li, Zetong Guan, Deming Chen, and Yingyan Lin. Autodnnchip: An automated dnn chip predictor and builder for both fpgas and asics. In *The 2020 ACM/SIGDA International Symposium on Field-Programmable Gate Arrays*, pages 40–50, 2020.
- [67] Xiaofan Zhang, Junsong Wang, Chao Zhu, Yonghua Lin, Jinjun Xiong, Wen-mei Hwu, and Deming Chen. Dnnbuilder: an automated tool for building high-performance dnn hardware accelerators for fpgas. In *2018 IEEE/ACM International Conference on Computer-Aided Design (ICCAD)*, pages 1–8. IEEE, 2018.
- [68] Junsong Wang, Qiuwen Lou, Xiaofan Zhang, Chao Zhu, Yonghua Lin, and Deming Chen. Design flow of accelerating hybrid extremely low bit-width neural network in embedded fpga. In *2018 28th International Conference on Field Programmable Logic and Applications (FPL)*, pages 163–1636. IEEE, 2018.
- [69] ARM. *AMBA AXI and ACE Protocol Specification*, 2013.
- [70] Xilinx, Inc. *Artix-7 FPGAs Data Sheet: DC and AC Switching Characteristics (DS181)*, 2018.
- [71] Xilinx, Inc. *Virtex-7 T and XT FPGAs Data Sheet: DC and AC Switching Characteristics (DS183)*, 2019.
- [72] Xilinx, Inc. *Zynq UltraScale+ MPSoC Data Sheet: DC and AC Switching Characteristics (DS925)*, 2019.
- [73] Power distribution network, 2015. <https://www.intel.com/content/www/us/en/programmable/support/support-resources/support-centers/signal-power-integrity/power-distribution-network.html>.
- [74] TI, Inc. *TPS54620 4.5-V to 17-V Input, 6-A, Synchronous, Step-Down SWIFT™ Converter*, 2017.
- [75] Xilinx, Inc. *UltraScale Architecture PCB Design (UG583)*, 2020.
- [76] Dennis RE Gnad, Fabian Oboril, and Mehdi B Tahoori. Voltage drop-based fault attacks on fpgas using valid bitstreams. In *2017 27th International Conference on Field Programmable Logic and Applications (FPL)*, pages 1–7. IEEE, 2017.
- [77] Kaspar Matas, Tuan Minh La, Khoa Dang Pham, and Dirk Koch. Power-hammering through glitch amplification—attacks and mitigation. In *2020 IEEE 28th Annual International Symposium on Field-Programmable Custom Computing Machines (FCCM)*, pages 65–69. IEEE, 2020.
- [78] Karen Simonyan and Andrew Zisserman. Very deep convolutional networks for large-scale image recognition. *arXiv preprint arXiv:1409.1556*, 2014.
- [79] Joseph Redmon and Ali Farhadi. Yolo9000: better, faster, stronger. *arXiv preprint*, 2017.
- [80] Alex Krizhevsky, Vinod Nair, and Geoffrey Hinton. Cifar-10 (canadian institute for advanced research). <http://www.cs.toronto.edu/kriz/cifar.html>, 2010.
- [81] Mark Sanderson. Christopher d. manning, prabhakar raghavan, hinrich schütze, introduction to information retrieval, cambridge university press. 2008. isbn-13 978-0-521-86571-5, xxi+ 482 pages. *Natural Language Engineering*, 16(1):100–103, 2010.
- [82] David G Mayer, BP Kinghorn, and Ainsley A Archer. Differential evolution—an easy and efficient evolutionary algorithm for model optimisation. *Agricultural Systems*, 83(3):315–328, 2005.
- [83] Kenneth V Price. Differential evolution. In *Handbook of Optimization*, pages 187–214. Springer, 2013.
- [84] Libiao Zhang, Xiangli Xu, Chunguang Zhou, Ming Ma, and Zhezhou Yu. An improved differential evolution algorithm for optimization problems. In *Advances in Computer Science, Intelligent System and Environment*, pages 233–238. Springer, 2011.
- [85] Swagatam Das, Sankha Subhra Mullick, and Ponnuthurai N Suganthan. Recent advances in differential evolution—an updated survey. *Swarm and Evolutionary Computation*, 27:1–30, 2016.

- [86] Feoktistov Vitaliy. Differential evolution—in search of solutions, 2006.
- [87] Model zoo: Discover open source deep learning code and pretrained models, 2019. <https://modelzoo.co>.
- [88] Vitis ai model zoo, 2018. <https://github.com/Xilinx/CHaiDNN/blob/master/docs/MODELZOO.md>.
- [89] Yukui Luo and Xiaolin Xu. A dynamic frequency scaling framework against reliability and security issues in multi-tenant fpga. In *2020 IEEE 28th Annual International Symposium on Field-Programmable Custom Computing Machines (FCCM)*, pages 210–210. IEEE, 2020.
- [90] Ognjen Glamočanin, Louis Coulon, Francesco Regazzoni, and Mirjana Stojilović. Are cloud fpgas really vulnerable to power analysis attacks? In *2020 Design, Automation & Test in Europe Conference & Exhibition (DATE)*, pages 1007–1010. IEEE, 2020.
- [91] Tsung-Yi Lin, Michael Maire, Serge Belongie, James Hays, Pietro Perona, Deva Ramanan, Piotr Dollár, and C Lawrence Zitnick. Microsoft coco: Common objects in context. In *European conference on computer vision*, pages 740–755. Springer, 2014.
- [92] Zhezhi He, Adnan Siraj Rakin, Jingtao Li, Chaitali Chakrabarti, and Deliang Fan. Defending and harnessing the bit-flip based adversarial weight attack. In *Proceedings of the IEEE/CVF Conference on Computer Vision and Pattern Recognition (CVPR)*, pages 14095–14103, 2020.
- [93] Vitis ai, 2020. <https://www.xilinx.com/products/design-tools/vitis/vitis-ai.html>.
- [94] Xilinx quantization, 2020. https://www.xilinx.com/html_docs/vitis_ai/1_2/modelquantization.html.
- [95] Mark Sandler, Andrew Howard, Menglong Zhu, Andrey Zhmoginov, and Liang-Chieh Chen. Mobilenetv2: Inverted residuals and linear bottlenecks. In *Proceedings of the IEEE Conference on Computer Vision and Pattern Recognition*, pages 4510–4520, 2018.
- [96] Chaidnn, hls based deep neural network accelerator library for xilinx ultrascale+ mpsoes. <https://github.com/Xilinx/CHaiDNN>, 2018.
- [97] Yolo-v2 pre-trained weight. <https://pjreddie.com/media/files/yolov2.weights>, 2016.
- [98] Lei Shan, Minxuan Zhang, Lin Deng, and Guohui Gong. A dynamic multi-precision fixed-point data quantization strategy for convolutional neural network. In *CCF National Conference on Computer Engineering and Technology*, pages 102–111. Springer, 2016.
- [99] Yolo2 accelerator in xilinx’s zynq-7000 soc. https://github.com/dhm2013724/yolov2_xilinx_fpga.
- [100] Di Wu, Yu Zhang, Xijie Jia, Lu Tian, Tianping Li, Lingzhi Sui, Dongliang Xie, and Yi Shan. A high-performance cnn processor based on fpga for mobilenets. In *2019 29th International Conference on Field Programmable Logic and Applications (FPL)*, pages 136–143. IEEE, 2019.